

1 SUPPLEMENTAL INFORMATION

2

3 SUPPLEMENTARY TEXT

4 **Properties of GRM encapsulation peptides (EPs)**

5 *Glycyl radical enzymes.* Secondary structure prediction of the putative N-terminal EPs of the
6 GRM1 GREs yielded two consecutive α -helices instead of just one as is typically found in the EPs of
7 other types of BMCs (1). Each of the helices is about 12 amino acids long. They are separated by ~4
8 residues predicted to be disordered, which may constitute a turn between the helices. A predicted
9 unordered ~30 amino acid long linker connects the two helices to the N-terminal domain of the GRE.
10 Similarly, secondary structure predictions for the insertion domains in the GRM3 and GRM5 GREs
11 yielded two central α -helices, ~15 residues each. The helices appear to be connected to one another via
12 a short (~5 residues) loop and are flanked by unordered, poorly conserved linkers (15 residues each on
13 average). In the case of the GRM3 GREs only the first of the two helices shows the characteristic
14 amphipathicity of EPs, whereas the second helix does not. Thus, the insertion in the GRM3 GREs
15 resembles the N-terminal extension of the GRM1 GREs. In contrast, in the GRM5 GREs both helices
16 of the insertion appear to be amphipathic. The GRM4 GREs provide yet another variation by
17 containing only one amphipathic α -helix of 15 residues length within this insertion.

18 *Aldehyde dehydrogenases.* The GRM1 and GRM2 AldDHs exhibit C-terminal extensions of
19 ~50-100 and ~80-100 residues, respectively. The characteristic predicted amphipathic helix of an EP is
20 found at the ends of these extension. In contrast, the GRM3-5 AldDHs contain N-terminal extensions
21 ranging from 30 up to 100 residues in length. These extensions exhibit the characteristics of EPs, *i.e.*
22 long flexible linkers (usually 10-20 residues) and predicted amphipathic α -helices of 12-15 residues
23 (1). Some GRM3 AldDHs (for example from *Rhodopseudomonas palustris* and *Rhodospirillum*
24 *rubrum*) contain two amphipathic helices (12-15 residues each), which are separated from one another

25 by long linkers (~20 residues) in the N-terminal extension. This type of EP resembles the ones found in
26 the GRM1, 3, and 5 GREs, which also comprise two α -helices and appears to be a unique feature of
27 GRMs in comparison to other characterized BMCs.

28

29 **Loci encoding GREs of Unknown Function (GUF)**

30 Genomes of the GRM1 encoding organisms *D. dehalogenans*, *D. hafniense* DCB-2 & Y51, and
31 *D. psychrophila* also contain an additional BMC gene cluster that we designate GUF loci. The GREs in
32 these loci do not contain any obvious EPs, and are oriented in the opposite direction of the rest of the
33 genes in the loci (except in *D. psychrophila*); all other known BMC loci encode their signature
34 enzymes and other components in the same orientation (2). Phylogenetically, the GUFs appear to be
35 more closely related to non-encapsulated GREs (Fig. 2A). Given these observations, we predict that
36 these GUFs are not packaged into BMCs. Nevertheless, the GUF loci appear to encode all other
37 required interior constituents of a functional BMC, with the exception of an alcohol dehydrogenase
38 gene. Interestingly, the GRM1 locus of *D. psychrophila* only encodes a non-functional AldDH,
39 whereas the GUF locus harbors genes for two (seemingly functional) AldDHs. They cluster together
40 with EutE from *Salmonella enterica*, the AldDH of the canonical EUT-BMC (Fig. 2D in the main text).
41 This is due to an apparent partial duplication within this GUF locus. All other GUF loci only encode
42 one functional AldDH, which phylogenetically cluster closely together with AldDHs of GRM1 loci.
43 Moreover, the GUF loci in *D. dehalogenans*, *D. hafniense* DCB-2 and Y51 only encode two BMC-Hs
44 (Dataset S1) meaning these GUF loci may not form functional organelles on their own. However, it is
45 possible that the genes in the GRM1 loci could complement the deficiencies of the GUF loci and their
46 co-expression results in a functional metabolosome. The situation appears to be reversed in *D.*
47 *psychrophila*, where the GRM1 locus lacks a BMC-P gene and only encodes a single BMC-H, whereas
48 the GUF locus encodes six BMC-Hs as well as a BMC-P. Collectively, these observations support the

49 hypothesis that cooperative expression of both GRM1 and GUF loci in *D. dehalogenans*, *D. hafniense*
50 DCB-2 & Y51, as well as *D. psychrophila* is required for the formation of a functional BMC.

51

52 **Locus type reclassifications**

53 As mentioned in the main text three loci (in *C. ljungdahlii*, *D. meridiei*, and *D. orientis*) that were
54 previously annotated as belonging to the GRM3 type (2) were re-classified as GRM1 based on the
55 phylogenetic analysis for the signature as well as the core enzymes. In detail, the GREs, the AEs, the
56 AldDHs, and the PTACs of the corresponding loci cluster together with their counterparts of the GRM1
57 loci in the respective phylogenetic trees. Moreover, the corresponding loci in *C. ljungdahlii*, *D.*
58 *meridiei* also encode an additional ‘dud’ AldDH. All three loci harbor a predicted choline/ethanolamine
59 kinase gene, further supporting their reclassification as GRM1 loci.

60

61 **Ancillary Enzymes/Proteins of GRM Loci**

62 In addition to signature and core enzymes, BMC loci typically encode additional
63 proteins/enzymes that are likely not directly involved in the degradation of a substrate, but instead
64 provide supporting functions, such as co-factor recycling, and integration of the BMC function with the
65 cytoplasm of the host and its environment (2, 3). These include genes encoding putative zinc-
66 containing alcohol dehydrogenases in GRM5 loci, acyl kinases in GRM3 loci, putative
67 S-adenosylmethionine synthetases in a subset of GRM3 loci, (putative) cobalamin reductases, a EutJ
68 homolog (in most GRM1 and GRM3 loci), and various putative metabolite transporters of the cell
69 membrane. Each GRM locus also appears to have its own (set of) transcription factor(s). The GRM1
70 loci encode a transcription factor of the MerR family, with a small molecule binding domain. GRM2
71 loci encode regulatory proteins of the TetR and LysR families. GRM3 and GRM4 loci encode

72 regulatory proteins of the PocR and AraC families with domains associated with two-component
73 signaling systems. GRM5 loci have a transcription factor of the DeoR family.

74

75 **Incomplete Shell Compositions of GRM Loci**

76 The GRM1 loci of *D. psychrophila* and *Clostridium tetani* lack genes encoding BMC-P
77 orthologs, the pentameric proteins that presumably cap the vertices of an icosahedral shell.
78 Furthermore, those two loci encode only one or two BMC-H proteins, respectively, which is a
79 relatively low number; the average number of genes encoding BMC-H proteins per BMC locus is 3.5
80 (2) and up to 5.5 for GRM1 loci. However, *D. psychrophila* also harbors a GUF locus containing two
81 BMC-P genes, an apparent duplication. It is, therefore, possible that in *D. psychrophila* the GUF locus
82 complements the GRM1 locus. However, no genes encoding BMC-Ps can be found anywhere in the
83 genome of *C. tetani* which otherwise has all of the GRM1 lumen protein genes intact.

84

85 **GRM fusion loci**

86 ***GRM1/GRM3 fusion.*** The two distinct GRM loci present in the genome of *C. ljungdahlii* may
87 instantiate an intermediate stage in the evolution of GRMs. It was surprising that the GRE and AE from
88 the two loci, fell within different phylogenetic clades (GRM1 or GRM3), while the AldDH and PTAC
89 from both loci were nested within the GRM1-associated clades. Upon closer inspection, it is apparent
90 that two sections of the locus that contained a gene encoding the choline TMA-lyase type GRE
91 (GRM1) had surprisingly high sequence identity (98%) with a large segment of the other locus
92 containing the propanediol dehydratase type GRE (Fig. S6). This duplication apparently includes genes
93 that are critical for GRM structure and function, such as those coding for BMC-H and BMC-P proteins,
94 an AldDH, as well as a PTAC. Given the phylogenetic distribution of the GRE, AE, AldDH and PTAC,
95 we inferred that a portion of a GRM1 locus was duplicated and inserted adjacent to an incomplete

96 GRM3 locus, thereby completing the locus as a whole structurally and enzymatically (Fig. S6). Two
97 genes in the duplicated region appear to have been lost; interestingly, one of them is a BMC-T protein
98 (Fig. S6). Since the incomplete GRM3 locus contained a BMC-T protein, it may be that the GRM1
99 BMC-T was redundant and eventually lost. Whether or not this hybrid GRM1/GRM3 locus is
100 functional can only be determined via experimentation. We expect that the GRM1-derived AldDH and
101 PTAC exhibit some promiscuity, accepting propionaldehyde and propionyl-CoA as substrates,
102 respectively (see Fig. 1B for comparison). Their enzymatic efficiency will likely improve over time due
103 to selective pressures. Based on the sequence identity, this duplication/transfer event must have
104 happened very recently, providing us a snapshot of a potential mechanism for functional divergence of
105 GRM loci.

106 ***PDU/GRM2 fusion.*** A PDU/GRM2 fusion locus in *Escherichia fergusonii* was found to contain
107 genes encoding a GRM2 GRE (see Fig. 2A), its activating enzyme, all of the subunits of a B₁₂-
108 dependent propanediol dehydratase, as well as two genes encoding PduL (phosphotransacylase)
109 homologs. One of these PduL homologs clusters together with GRM2 PTACs, whereas the other one
110 was closely related to PduL from the PDU locus of *Salmonella enterica* (Fig. 2E). These observations
111 may indicate that this PDU/GRM2 locus has a dual-function, being used for the simultaneous
112 degradation of propanediol and choline.

113

114 **SUPPLEMENTAL REFERENCES**

115

116 1. **Aussignargues C, Paasch BC, Gonzalez-Esquer R, Erbilgin O, Kerfeld CA.** 2015. Bacterial
117 Microcompartment Assembly: The Key Role of Encapsulation Peptides. *Commun Integr Biol*
118 **8:e1039755.**

119 2. **Axen SD, Erbilgin O, Kerfeld CA.** 2014. A Taxonomy of Bacterial Microcompartment Loci
120 Constructed by a Novel Scoring Method. *PLoS Comput Biol* **10.**

121 3. **Kerfeld CA, Erbilgin O.** 2015. Bacterial microcompartments and the modular construction of
122 microbial metabolism. *Trends Microbiol* **23:22-34.**

123

Table S1. BMC associated glycy radical enzymes included in this study

Species	Locus type	Accession
<i>Alkaliphilus metalliredigens</i> QYMF	GRM1	YP_001321612
<i>Alkaliphilus oremlandii</i> OhILAs	GRM1	YP_001513926
<i>Clostridium botulinum</i> A str. ATCC 3502	GRM1	YP_001254614
<i>Clostridium botulinum</i> A3 str. Loch Maree	GRM1	YP_001787508
<i>Clostridium botulinum</i> B str. Eklund 17B	GRM1	YP_001885647
<i>Clostridium botulinum</i> B1 str. Okra	GRM1	YP_001781665
<i>Clostridium botulinum</i> Ba4 str. 657	GRM1	YP_002863094
<i>Clostridium botulinum</i> BKT015925	GRM1	YP_004396407
<i>Clostridium botulinum</i> E3 str. Alaska E43	GRM1	YP_001920768
<i>Clostridium botulinum</i> F str. Langeland	GRM1	YP_001391412
<i>Clostridium botulinum</i> H04402 065	GRM1	YP_005678666
<i>Clostridium phytofermentans</i> ISDg	GRM1	YP_001558531
<i>Clostridium saccharolyticum</i> WM1	GRM1	YP_003824152
<i>Clostridium tetani</i> E88	GRM1	NP_782070
<i>Desulfotobacterium dehalogenans</i> ATCC 51507	GRM1	YP_006432251
<i>Desulfotobacterium hafniense</i> DCB-2	GRM1	YP_002461335
<i>Desulfotobacterium hafniense</i> Y51	GRM1	YP_521239
<i>Desulfosporosinus acidiphilus</i> SJ4	GRM1	YP_006465906
<i>Desulfotalea psychrophila</i> LSv54	GRM1	YP_065559
<i>Desulfotomaculum reducens</i> MI-1	GRM1	YP_001114603
<i>Desulfotomaculum ruminis</i> DSM 2154	GRM1	YP_004545628
<i>Desulfovibrio alaskensis</i> G20	GRM1	YP_389771
<i>Desulfovibrio desulfuricans</i> ATCC 27774	GRM1	YP_002479937
<i>Desulfovibrio hydrothermalis</i> AM13	GRM1	YP_007325732
<i>Desulfovibrio salexigens</i> DSM 2638	GRM1	YP_002990074
<i>Olsenella uli</i> DSM 7084	GRM1	YP_003800310
<i>Streptococcus dysgalactiae</i> ATCC 12394	GRM1	YP_006013997
<i>Streptococcus dysgalactiae</i> RE378	GRM1	YP_006860442
<i>Streptococcus iniae</i> SF1	GRM1	YP_008055971
<i>Streptococcus intermedius</i> ATCC 27335	GRM1	EPH05251
<i>Streptococcus intermedius</i> JTH08	GRM1	YP_006469536
<i>Clostridium ljungdahlii</i> DSM 13528	GRM1*	YP_003782109
<i>Desulfosporosinus meridiei</i> DSM 13257	GRM1*	YP_006624072
<i>Desulfosporosinus orientis</i> DSM 765	GRM1*	YP_004973312
<i>Aeromonas hydrophila</i> ML09-119	GRM2	YP_008042577
<i>Aeromonas hydrophila</i> ATCC 7966	GRM2	YP_855870
<i>Enterobacter aerogenes</i> KCTC 2190	GRM2	YP_004592209
<i>Escherichia coli</i> 536	GRM2	YP_672437
<i>Escherichia coli</i> IAI39	GRM2	YP_002410085

<i>Escherichia coli</i> O7:K1 str. CE10	GRM2	YP_006146235
<i>Escherichia coli</i> UTI89	GRM2	YP_543898
<i>Klebsiella oxytoca</i> E718	GRM2	YP_006496423
<i>Klebsiella oxytoca</i> KCTC 1686	GRM2	YP_005017919
<i>Klebsiella pneumoniae</i> 342	GRM2	YP_002240668
<i>Klebsiella variicola</i> At-22	GRM2	YP_003441426
<i>Proteus mirabilis</i> HI4320	GRM2	YP_002152417
<i>Raoultella ornithinolytica</i> B6	GRM2	YP_007875383
<i>Serratia marcescens</i> FGI94	GRM2	YP_007343022
<i>Shimwellia blattae</i> DSM 4481	GRM2	YP_006318380
<i>Vibrio furnissii</i> NCTC 11218	GRM2	YP_004991566
<i>Clostridium beijerinckii</i> NCIMB 8052	GRM3	YP_001311127
<i>Clostridium cf. saccharolyticum</i> K10	GRM3	YP_007849774
<i>Clostridium ljungdahlii</i> DSM 13528	GRM3	YP_003779353
<i>Clostridium novyi</i> NT	GRM3	YP_878969
<i>Escherichia coli</i> APEC O1	GRM3	YP_859768
<i>Escherichia coli</i> CFT073	GRM3	NP_756397
<i>Escherichia coli</i> ED1a	GRM3	YP_002399331
<i>Escherichia coli</i> S88	GRM3	YP_002394164
<i>Oscillibacter valericigenes</i> Sjm18-20	GRM3	YP_004881456
<i>Pectobacterium wasabiae</i> WPP163	GRM3	YP_003261427
<i>Raoultella ornithinolytica</i> B6	GRM3	YP_007872971
<i>Rhodobacter capsulatus</i> SB 1003	GRM3	YP_003578348
<i>Rhodospseudomonas palustris</i> BisB18	GRM3	YP_531045
<i>Rhodospirillum rubrum</i> ATCC 11170	GRM3	YP_425991
<i>Rhodospirillum rubrum</i> F11	GRM3	YP_006047199
<i>Vibrio sp.</i> EJY3	GRM3	YP_005023152
<i>Shewanella putrefaciens</i> CN-32	GRM4	YP_001181743
<i>Shewanella sp.</i> W3-18-1	GRM4	YP_961832
<i>Clostridium phytofermentans</i> ISDg	GRM5	YP_001558291
<i>Roseburia inulinivorans</i> DSM 16841	GRM5	EEG94456
<i>Ruminococcus obeum</i> A2-162	GRM5	YP_007805196
<i>Ruminococcus sp.</i> SR1/5	GRM5	YP_007783755
<i>Ruminococcus torques</i> L2-14	GRM5	YP_007786118
<i>Desulfotobacterium dehalogenans</i> ATCC 51507	GUF#	YP_006428626
<i>Desulfotobacterium hafniense</i> DCB-2	GUF#	YP_002456869
<i>Desulfotobacterium hafniense</i> Y51	GUF#	YP_516649
<i>Desulfotalea psychrophila</i> LSv54	GUF#	YP_066763
<i>Escherichia fergusonii</i> ATCC 35469	PDU/GRM	YP_002383121

*Reclassified, previously GRM3. #Reclassified, previously GRM1.

Table S2. GRM loci lacking genes encoding the iron-containing type of alcohol dehydrogenase (pfam00465).

GRM loci types	Species
GRM1	<i>Desulfosporosinus acidiphilus</i> SJ4
GRM1 (GRM3 outlier)	<i>Clostridium ljungdahlii</i> DSM 13528
GRM1 (GRM3 outlier)	<i>Desulfosporosinus meridiei</i> DSM 13257
GRM1 (GRM3 outlier)	<i>Desulfosporosinus orientis</i> DSM 765
GRM1 & GUF	<i>Desulfitobacterium dehalogenans</i> ATCC 51507
GRM1 & GUF	<i>Desulfitobacterium hafniense</i> DCB-2
GRM1 & GUF	<i>Desulfitobacterium hafniense</i> Y51
GRM1 & GUF	<i>Desulfotalea psychrophila</i> LSv54
GRM2	<i>Escherichia coli</i> IAI39
GRM5	<i>Clostridium phytofermentans</i> ISDg
GRM5	<i>Roseburia inulinivorans</i> DSM 16841

SUPPLEMENTAL FIGURE LEGENDS

Figure S1. GRE active site comparisons. A.) Stereo view superposition of a GRM3 GRE (*R. palustris* BisB18) homology model with the crystal structure of the glycerol-bound form of the B₁₂-independent glycerol dehydratase (GDH) (PDB 1R9D). GRM3 GRE residues that are divergent from the ones in the GDH are colored in orange. The other residues are conserved in both active sites. Residues are numbered according to the GDH structure. Cysteine 433 is the residue that harbors the radical during catalysis. Serine 642 is replaced by a valine residue in all GRM3, GRM4, and GRM5 GREs. This valine would form an unfavorable short contact to the hydroxyl group of glycerol. This hydroxyl group is absent in propanediol. Tyrosine 339 of the GDH is replaced by a phenylalanine in all the GRE3-5, providing a more hydrophobic for the terminal methyl group of propanediol together with the conserved valine residue. **B.)** Stereo view superposition of homology models for the GRM1 GRE choline trimethylamine-lyase (CHL) from *D. alaskensis* G20 (blue) and the GUF of *D. hafniense* Y51 (orange). The first letters and the numbering correspond to the residues of the CHL. The second letters represents the residues that differ in the GUF. All residues shown are in close proximity to the catalytic radical cysteine (C489 in the CHL), and are conserved in the CHLs or GUFs, respectively. The only exception is threonine 431, which can be replaced by serine in some of the GRM1 GREs.

Figure S2. Homology model of the GRM2 GRE and schematics of possible protein interactions.

A.) Dimer of the B₁₂-independent glycerol dehydratase (GDH) (PDB 1R9D). **B.)** Homology model (created with RaptorX) of the GRM2 GRE that includes the N-terminal ~350 residues long extension (outlined in red). The modeled extension resembles the first part of the catalytic domain of the GRE (outlined in yellow). The latter is shown in the same orientation as the dark blue subunit of the GDH in panel A. **C.)** Schematic for a possible coalescence of the GRM2 GRE within the microcompartment.

The coalescence may be facilitated by the N-terminal partial catalytic domain, by replacing another catalytic domain in the dimer interface. **D.)** Schematic for a possible role of the N-terminal extension domain in the interaction with the BMC shell, similar to encapsulation peptides. Note that in contrast to the other BMC associated GREs, the GRM2 GREs do not contain any apparent encapsulation peptides.

Figure S3. Alignment of the insertion domains within the activating enzymes containing additional Fe-S cluster motifs. Sequence alignment used to construct the phylogeny of the activating enzymes (Figure 2B) depicting the insertion domains that comprise the ferredoxin-like [4Fe-4S] cluster motifs. Cysteine residues are highlighted in orange. Species names and GRM classifications are provided on the left, whereas the total number of [4Fe-4S] clusters present in the respective activating enzyme is noted on the right.

Figure S4. Phylogenetic tree for the GRM prevalent iron containing type of alcohol dehydrogenases (ADHs). The Maximum Likelihood tree of the ADHs was inferred from 67 amino acid sequences. The counterparts from the canonical PDU and EUT BMCs, PduQ and EutG, respectively, have been included for comparison. Bootstrap values for important nodes are represented as filled circles (above 50%) and empty circles (below 50%).

Figure S5. Phylogenetic trees of BMC-H, BMC-T and BMC-P shell proteins

Maximum Likelihood trees of the BMC-H, BMC-T, and BMC-P proteins were inferred from 354, 67 and 82 amino acid sequences, respectively. Bootstrap values for important nodes are represented as filled circles (above 50%) and empty circles (below 50%).

Figure S6. Proposed evolution of the *C. ljungdahlii* GRM locus. The borders of duplication and deletion were determined based on dot plot analysis (Figure S1). The order of operations was inferred based on the observation that the PduL homolog and AldDH in both loci were nested within the GRM1 clades in their respective phylogenetic trees. CHL – choline trimethylamine-lyase, PDH - propanediol dehydratase.

SUPPLEMENTAL FIGURES

Figure S1

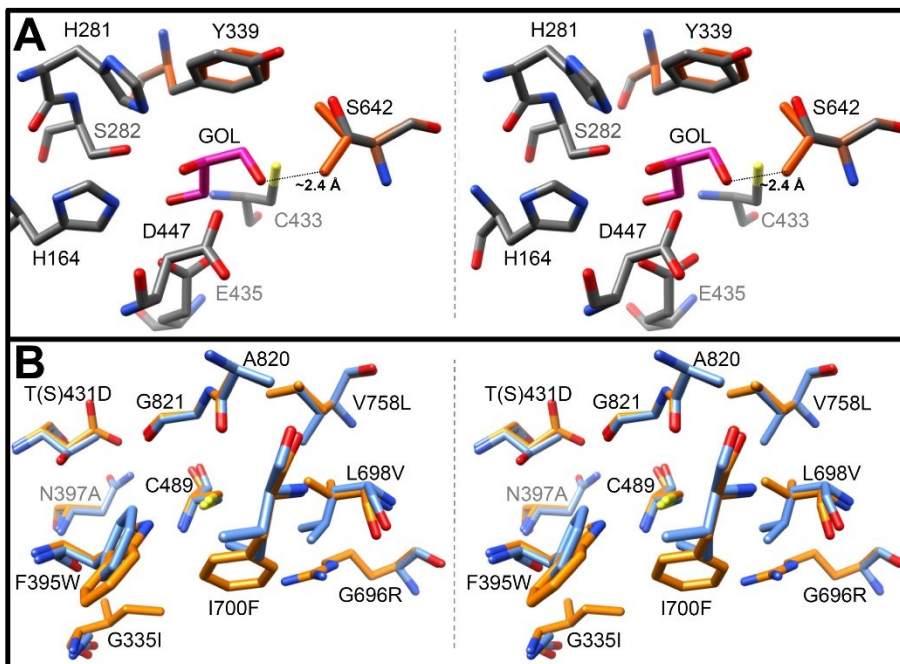


Figure S2.

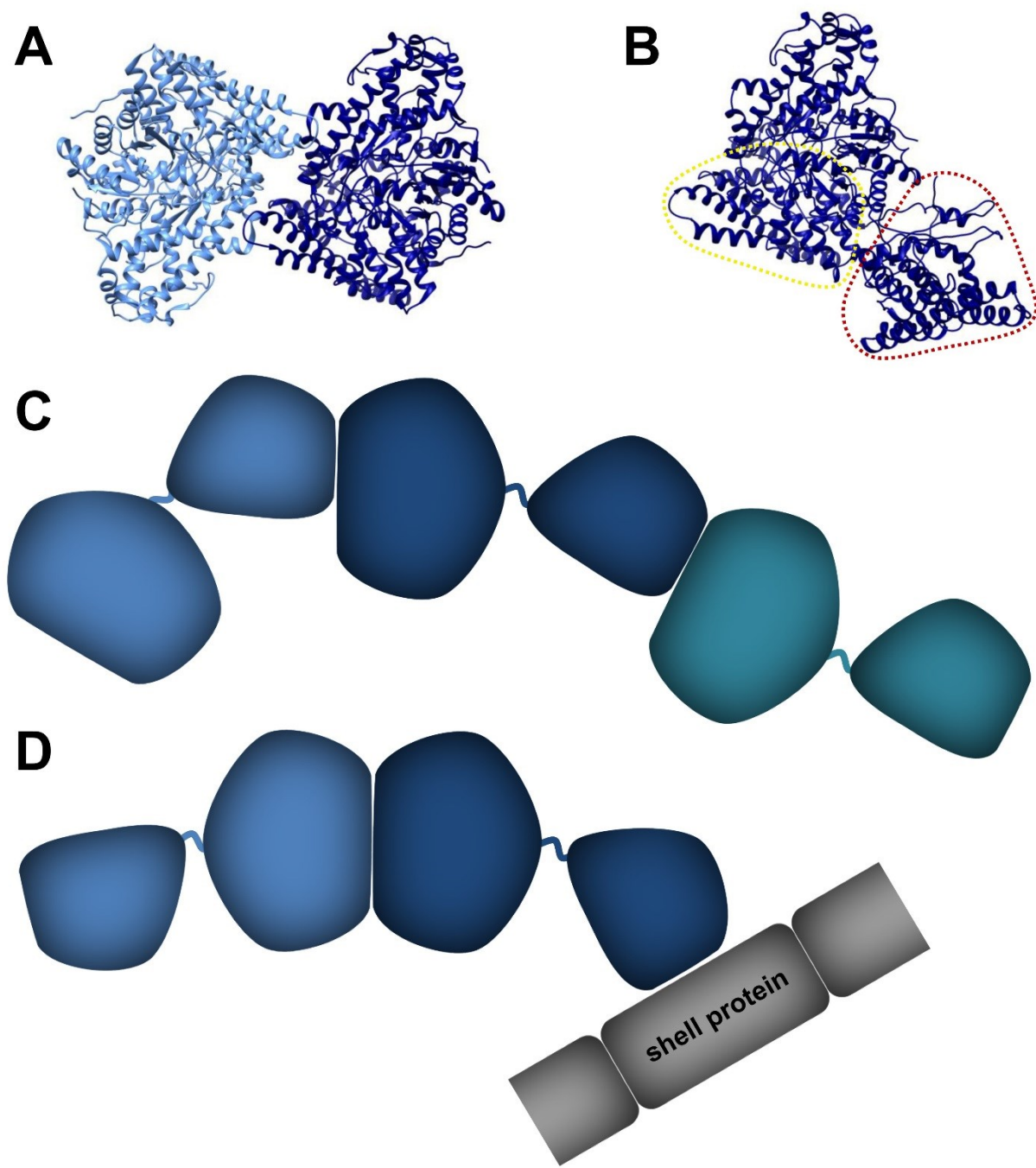


Figure S3.

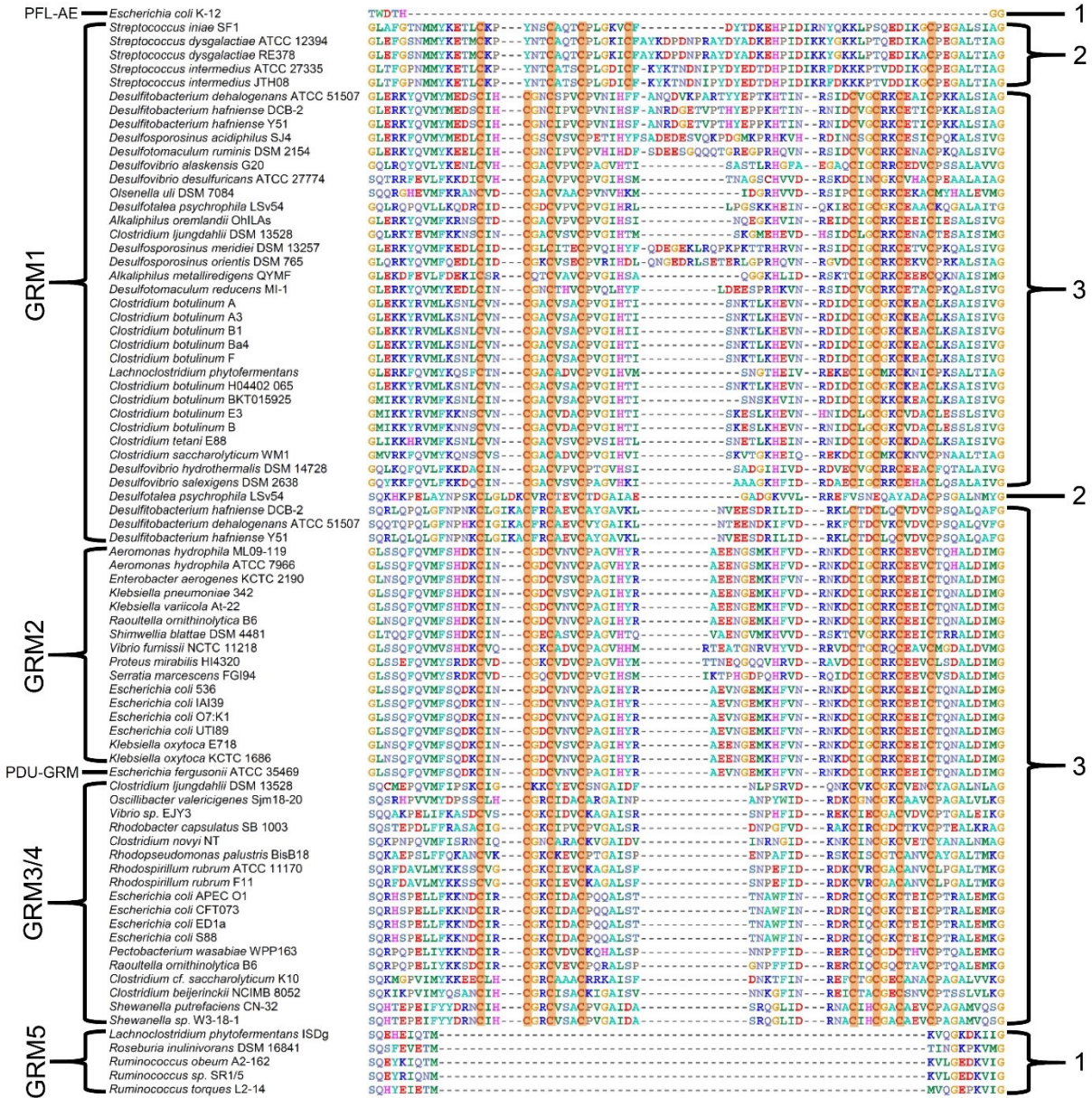


Figure S4.

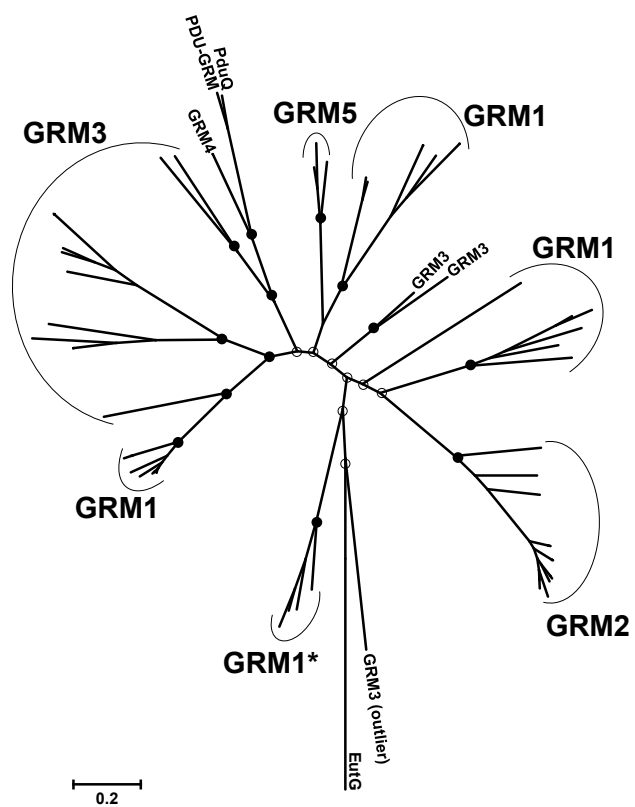
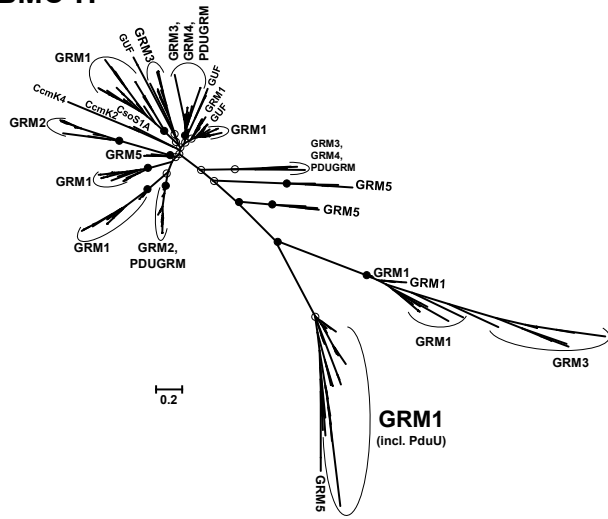
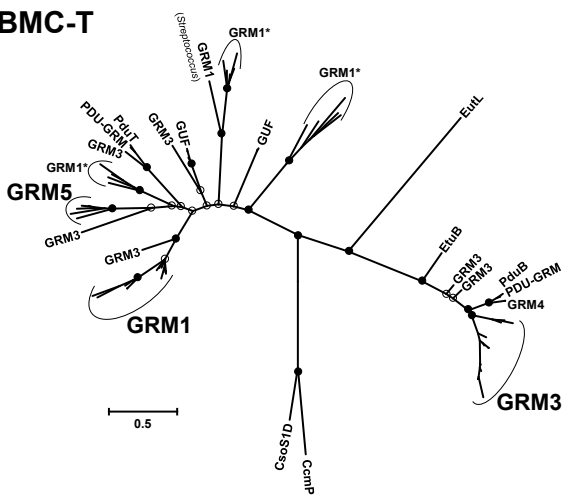


Figure S5.

BMC-H



BMC-T



BMC-P

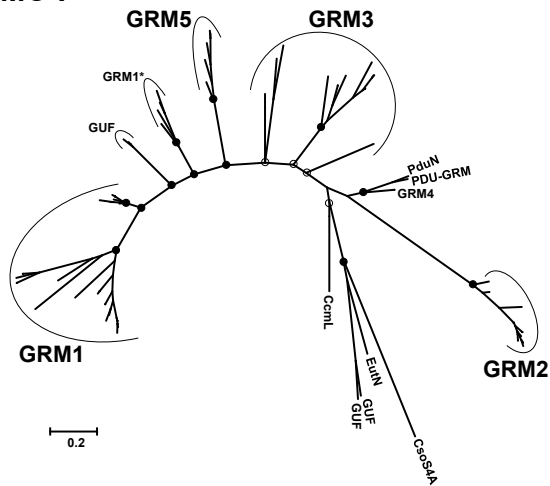


Figure S6.

